Ultimately, one wishes to separately encapsulate individual scintillator beads. Thus, the procedure described has the advantages of simplicity, but the encapsulated scintillator used here is only a crude approximation of the ideal (Figure 2). We are currently exploring alternative procedures for encapsulation and detection.

Finally, it is noted that many cells or cell clusters are substantially larger than a few micrometers across. If the tritiated solute is incorporated into the bulk of such an object, then the object can act as its own shield for large fractions of its internal volume. For example, 73% of the volume of a spherical cell 10 μm in diameter is more than 1 μm removed from the cell surface. In such cases, uncoated scintillator microspheres, when mixed with the cell suspension, will monitor the bulk absorption of the tritiated solute with kinetics limited only by the time required for the solute to be incorporated into the cell.

Acknowledgments

We are grateful to Geo T. Reynolds, J. R. Milch, M. L. Applebury, J. Karohl, and D. T. Barry for helpful discussions. We also thank Dr. M. Garcia for help with the *E. coli* vesicle experiments.

References

Birks, J. B. (1964) *The Theory and Practice of Scintillation Counting*, Pergamon Press, New York.
Felle, H., Porter, J. S., Slayman, C. L., & Kaback, H. R. (1980) *Biochemistry 19*, 3585.
Kaback, H. R. (1971) *Methods Enzymol. 31*, 99.
Kirk, G., & Gruner, S. M. (1982) *IEEE Trans. Nucl. Sci. NS-29*, 769.
Ramos, S., & Kaback, H. R. (1977) *Biochemistry 16*, 848.
Ramos, S., Schuldiner, S., & Kaback, H. R. (1976) *Proc. Natl. Acad. Sci. U.S.A. 73*, 1892.
Ramos, S., Schuldiner, S., & Kaback, H. R. (1979) *Methods Enzymol. 55*, 680.
Schuldiner, S., & Kaback, H. R. (1975) *Biochemistry 14*, 5451.
Short, S. A., Kaback, H. R., & Kohn, L. D. (1975) *J. Biol. Chem. 250*, 4291.
Weast, R. C., Ed. (1970) *CRC Handbook of Chemistry and Physics*, 51st ed., p F-47, CRC Press, Cleveland, OH.
Zaborsky, O. R., Ed. (1973) *Immobilized Enzymes*, CRC Press, Cleveland, OH.

Conformation of the Deoxydinucleoside Monophosphate dCpdG Modified at Carbon 8 of Guanine with 2-(Acetylamino)fluorene†

B. Hingerty and S. Broyde*

ABSTRACT: Minimized conformational potential energy calculations were performed for dCpdG modified with the carcinogen 2-(acetylamino)fluorene (AAF). The major adduct, linked via a covalent bond between guanine C-8 and N-2 of AAF, was investigated. The 12 variable torsion angles and both deoxyribose puckers were independent flexible parameters in the energy minimizations. Three categories of low-energy conformers were calculated in which the guanine was syn and nearly perpendicular to the plane of the fluorene: (1) forms in which fluorene is stacked with cytidine (included among these is the global minimum energy conformation); (2) conformers which preserve guanine–cytidine stacking while placing the fluorene in a base-pair obstructing position; (3) conformers which maintain guanine–cytidine stacking and place the fluorene at the helix exterior, without interfering with base pairing. The Z form is important in this group. In addition, a low-energy conformation with guanine anti, but still nearly perpendicular to fluorene, was computed. Molecular models were constructed for the most important conformations incorporated into larger polymers. These indicated that the fluorene–cytidine stacked forms induce a severe kink in the B helix. Conformers with guanine–cytidine stacking and AAF in a base-pair obstructing position place the AAF at the B-type helix interior with little distortion in the helix direction. Conformers with the guanine–cytidine stack in which AAF does not affect base pairing place the fluorene at the Z or alternate helix exterior. It is suggested that base sequence, extent of modification, and external conditions such as salt concentration determine which of a number of possible conformational effects is actually induced by AAF. The variety of observed experimental results with AAF-modified DNA may reflect these various conformational possibilities.

The carcinogen *N*-acetoxy-2-(acetylamino)fluorene (AAAF) links covalently to DNA. In vitro, the major adduct (about 80%) results from a linkage between C-8 of guanine and N-2 of AAAF (Kriek et al., 1967), while a minor adduct results from a linkage between N-2 of guanine and C-3 of AAAF (Kriek, 1972; Westra et al., 1976; Yamasaki et al., 1977). The acetoxy is eliminated, yielding the products C8(G)-N2(AAF) and N2(G)-C3(AAF). In vivo these same two adducts are observed (Kriek, 1972), but a large fraction of the C8(G) adducts are deacetylated to give C8(G)-N2(AF) (Irving & Veazey, 1969; Kriek, 1972, 1974; Kriek & Westra, 1980). Uncharacterized adenine adducts, present in small amounts, have also been reported in vitro (Kapuler & Michelson, 1971; Kriek & Rietsema, 1971; Levine et al., 1974). In vivo, the major C8(G)-N2(AAF) adduct is largely repaired, while the minor N2(G)-C3(AAF) adduct is persistent (Howard et al., 1981, and references cited therein).

A great deal of experimental work has been done in an effort

† From the Biology Division, Oak Ridge National Laboratory, Oak Ridge, Tennessee 37830 (B.H.), and the Biology Department, New York University, New York, New York 10003 (S.B.). *Received December 18, 1981.* This work was supported jointly by BRSG Grant RR07062, awarded by the Biomedical Research Support Grant Program, Division of Research Resources, National Institutes of Health (S.B.), by American Cancer Society Institutional Grant IN-14V to New York University (S.B.), by National Institutes of Health Grant 1 R01 CA28038-01A1 (S.B.), by Department of Energy Contract DE-AC02-81 ER60015 (S.B.), and by the Office of Health and Environmental Research, U.S. Department of Energy, under Contract W-7405-eng-26 with the Union Carbide Corp. (B.H.). A grant of computer time on the CDC 6600 at the Courant Institute of New York University, supported by the U.S. Department of Energy, Division of Basic Energy Sciences, Applied Mathematical Sciences Program under Contract DE-AC02-76ER03077, is gratefully acknowledged.

0006-2960/82/0421-3243$01.25/0

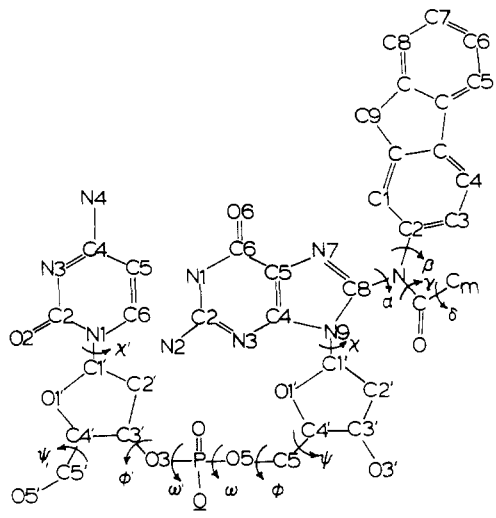

FIGURE 1: Structure, numbering scheme, and variable conformational angle designations for dCpdG-C8(G)-N2(AAF). The dihedral angles A–B–C–D are defined as follows: χ', O-1′–C-1′–N-1–C-6; χ, O-1′–C-1′–N-9–C-8; ψ_1,ψ, C-3′–C-4′–C-5′–O-5′; ϕ', P–O-3′–C-3′–C-4′; ϕ, C-4′–C-5′–O-5′–P; ω', O-5′–P–O-3′–C-3′; ω, C-5′–O-5′–P–O-3′; α, N-9–C-8–N–C-2; β, C-8–N–C-2–C-1; γ, C-8–N–C–Cm; δ, N–C–Cm–H. The angle A–B–C–D is measured by a clockwise rotation of D with respect to A, looking down the B–C bond. A eclipsing D is 0°. Sugar pucker in the calculations is defined by the pseudorotation parameter P (Altona & Sundaralingam, 1972). P_1 is 5′ linked; P_2 is 3′ linked.

to elucidate the conformational influence of AAF modification on DNA. These results are primarily applicable to the major adduct whose characteristics predominate. Circular dichroism (CD) and NMR studies with dinucleoside monophosphates, as well as model building, have led to the base displacement model, in which the guanine is rotated to the syn position, causing the fluorene ring to stack with the adjacent base while removing the guanine from its previous stacked location (Grunberger & Weinstein, 1979; Grunberger et al., 1970). A series of experiments with AAF-modified DNA polymer, including melting and formaldehyde unwinding studies, S1 nuclease digestion (specific for single-stranded regions), electric dichroism measurements, and hydrodynamic studies involving light scattering and viscosity measurements, have also been carried out (Fuchs & Daune, 1972, 1974; Fuchs, 1975; Fuchs et al., 1976). A conformational model termed insertion–denaturation has resulted from this work. In this model, the fluorene is inserted between adjacent bases, the guanine is syn, and base pairing is interrupted. Base displacement and insertion–denaturation are viewed as analogous models, but conformational details on how these distortions can be achieved are not available. Recently, with the finding that duplex poly(dC-dG) can adopt a left-handed conformation termed Z-DNA (Wang et al., 1981), experiments have been undertaken to determine if AAF can induce the Z form, in which the guanine is already syn, in this base sequence. CD studies, S1 nuclease digestion experiments, and investigation of reactivity with anti-cytidine antibodies have shown that AAF causes poly(dC-dG)·poly(dC-dG) to adopt a left-handed form with base pairs intact (Sage & Leng, 1980; Santella et al., 1981a; Grunberger & Santella, 1981). This structure is presumed to be the Z form. Again, conformational details are not available.

In order to learn how covalently linked aminofluorenes alter the conformation of DNA, we have made minimized conformational potential energy calculations for modified deoxydinucleoside monophosphates. In the present work we report results for the first in a series of studies. For this investigation we chose the major adduct of AAF with dCpdG, that is, dCpdG-C8(G)-N2(AAF) (Figure 1). We have found three different classes of low-energy conformations with guanine syn. The types of syn conformers are (1) forms with fluorene–cytidine stack, (2) forms with guanine–cytidine stack and fluorene in a base-pair obstructing position, and (3) forms with AAF at the helix exterior, where its orientation is flexible. The Z form is an important member of this class. These classes are each represented by a number of conformers which are similar in overall aspect, although the class members are very different in DNA conformational detail. In addition, a single low-energy conformer with guanine anti has been computed. Some preliminary results of this work have been presented (Broyde & Hingerty, 1981, 1982; Santella et al., 1981b).

Methods

Figure 1 gives the structure, numbering scheme, and torsion angle definitions for dCpdG-C8(G)-N2(AAF).

A number of improvements to our potential functions (Broyde et al., 1978) have been made in the present study. These follow the works of Srinivasan and co-workers (1980), Srinivasan & Olson (1980), and Olson (1982), by including anomeric potentials for phosphate and deoxyribose, a long-range Coulombic screening term, and a method to approximate counterion condensation, in addition to the terms used previously (Broyde et al., 1978).

The energy of the molecule is calculated by

$$E = E_{nb} + E_{el} + E_{tor} + E_{an} + E_{st} \quad (1)$$

The nonbonded term, E_{nb}, is the usual Leonard–Jones potential

$$E_{nb} = \sum_{i<j}\sum(a_{ij}r_{ij}^{-6} + b_{ij}r_{ij}^{-12}) \quad (2)$$

with parameters a and b taken from Lakshminarayanan & Sasisekharan (1969a). The a's and b's are modified so that the distance of closest approach of two atoms is the sum of the van der Waals radii plus 0.2 Å. The electrostatic term, E_{el}, is the standard coulomb potential modified with an exponential screening term

$$E_{el} = \sum_{i<j}\sum(332q_iq_je^{-\beta r_{ij}})/(\epsilon r_{ij}) \quad (3)$$

The partial charges q_i for DNA are taken from Ornstein & Rein (1979) except for the free 3′ and 5′ OH groups for which the earlier values of Renugopalakrishnan et al. (1971) were employed, since these free ends were not present in Ornstein and Rein's structures. Preliminary calculations for dCpdG indicated that the two sets of charges led to very similar minima. Partial charges assigned to the ionized phosphate oxygens were reduced to −0.162 following Srinivasan & Olson (1980), to approximate the presence of counterions. Partial charges for the fluorene moiety, including the linkage site, were computed by the INDO method, with a program kindly supplied by Professor Graham Underwood. Since only 80 orbitals could be accommodated in the program, the structure was computed in overlapping pieces (guanine, linkage site and adjacent rings, fluorene), and the values at the edges were averaged. Partial charges computed for guanine were very similar to those of Ornstein & Rein (1979), which are used for the adduct except at N-7, C-8, and N-9. Results are shown in Figure 2. β and ϵ, the dielectric constant, were assigned values of 0.1 (Srinivasan & Olson, 1980) and 4, respectively.

The intrinsic torsional contribution to the energy, E_{tor}, is given by

$$E_{tor} = \sum_{k=1}^{n}(V_{0,k}/2)[1 \pm \cos(m\theta_k)] \quad (4)$$

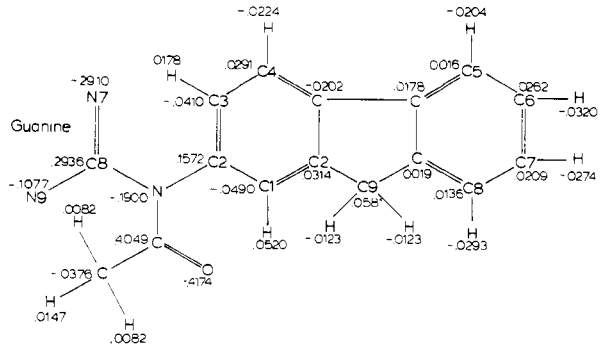

FIGURE 2: Partial charges computed for AAF and linkage vicinity.

Table I: Intrinsic Torsion Barriers Employed in Equation 4

torsion angle (deg)	V_0 (kcal/mol)	sign	m	reference
χ',χ	0	+	3	Lakshminarayanan & Sasisekharan (1969b)
ϕ',ϕ	2.0	+	3	Lakshminarayanan & Sasisekharan (1969b)
ψ_1,ψ	2.8	+	3	Srinivasan & Olson (1980)
ω',ω	1.0	+	3	Srinivasan & Olson (1980)
α	3.54	−	2	Evans (1960)
β	3.54	−	2	Evans (1960)
γ	20.0	−	2	Momany et al. (1975)
δ	−1.34	+	3	Kao & Allinger (1977)
C–C (deoxyribose)	2.53	+	3	T. Sato (unpublished results)
C–O (deoxyribose)	1.03	+	3	T. Sato (unpublished results)

where n is the number of flexible torsional rotations, m is 1, 2, or 3 with the cosine term added or subtracted, depending on the nature of the given rotation, and θ_k is the instantaneous value of the torsion angle. Table I gives the intrinsic torsion barriers, V_0, the sign of the cosine term, and m for each flexible bond. Barriers for the nucleic acids follow previous assignments. For the AAF linkage site, however, proper barriers had to be chosen. Aniline was chosen as a reasonable model for the C–N rotations α and β, and the 2-fold barrier to internal rotation about C–N computed from Raman and infrared spectra of aniline (Evans, 1960) was assigned to these torsions. The high 2-fold barrier employed in peptide linkages (Momany et al., 1975) was assigned to γ. The threefold barrier computed by Kao & Allinger (1977) for the $H–C_{sp^3}–C_{sp^2}–C_{sp^2}$ rotation was assigned to δ, taking N as analogous to C_{sp^2}.

The anomeric correction terms for the phosphate, following Srinivasan & Olson (1980), are

$$E_{an,P} = (0.4/2)[1 - \cos(2\psi)] + (1.3/2)[1 - \cos[2(\psi - 120)]] + (2.8/2)(1 + \cos\phi) \quad (5)$$

where ψ is the C-3′–C-4′–C-5′–O-5′ torsion angle and ϕ is the dihedral angle between the lone pair electrons on the O-3′ and O-5′ surrounding P.

Anomeric correction terms for deoxyribose (Olson, 1982) are

$$E_{an,r} = \sum_{i=1}^{m}(V_{0,an}/2)[1 + \cos(2\theta_i)] \quad (6)$$

where the θ_i are the dihedral angles defined by the m C–C–C–O and O–C–C–O rotations (including pendant atoms) associated with the deoxyribose, and $V_{0,an}$ and the barrier heights of 0.2 and 1 kcal/mol for these two types of rotations, respectively.

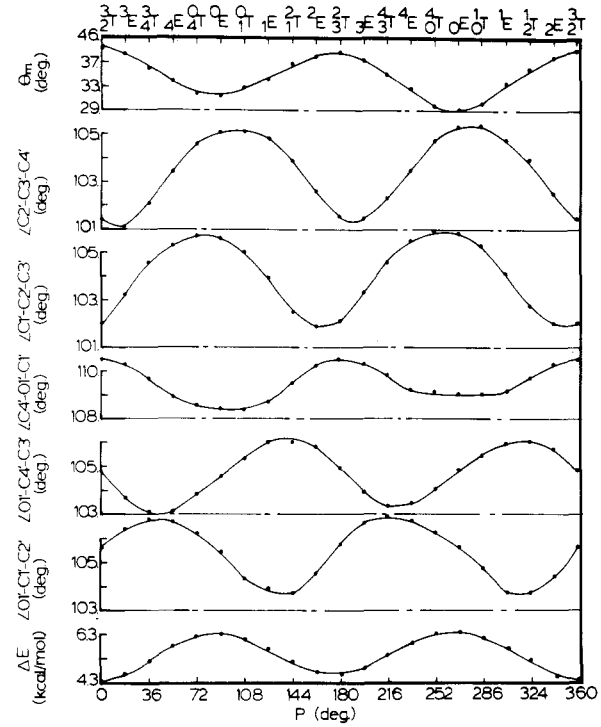

FIGURE 3: Energy, ΔE, bond angles, and puckering amplitude, θ_m, as a function of pseudorotation parameter P. T = twist; E = envelope conformation. Upper and lower numbers are endo and exo atoms, respectively.

Finally, a strain term for each of the five deoxyribose bond angles was included, as in previous work (Broyde et al., 1978). This is of the form

$$E_{st} = \sum_{i=1}^{5} K_\tau(\tau - \tau_0)^2 \quad (7)$$

where τ is the instantaneous bond angle value, τ_0 is the equilibrium value of the bond angle, and K_τ is the force constant. The τ_0 values are 113.5°, 110.0°, and 109.5°, and the K_τ values [kcal/(mol·rad^2)] are 66.5, 59.5, and 54.0 for C–O–C, C–C–O, and C–C–C, respectively. The energy of deoxyribose was calculated earlier by Sato (Sasisekharan, 1973) from eq 2, 3 (without the exponential screening term), 4, and 7, as a function of the pseudorotation parameter, P (Altona & Sundaralingam, 1972), puckering amplitude θ_m, and bond angles O-1′–C-1′–C-2′ and O-1′–C-4′–C-3′. His results for these bond angles have been shifted in phase such that $P_{old} + P_{new} = 216°$, which now results in an excellent match between experimental and theoretical values for the bond angles (Olson, 1982). The energies, bond angles, and θ_m for deoxyribose incorporated in the present work are shown in Figure 3. Linear interpolation of these values permitted a continuous variation of deoxyribose conformation.

Coordinates of the molecules were generated via the linked atom algorithm of Scott & Scheraga (1966), using bond lengths and bond angles given by Arnott et al. (1969) for the nucleic acid moiety. They were invariant except for the deoxyribose bond angles described above. The pendant 3′ and 5′ oxygens were assigned geometries identical with their phosphorus-linked analogues. Bond lengths and angles for fluorene were taken from the crystal structure of Burns & Iball (1955). Reasonable bond length and angle assignments for the linkage site are shown in Figure 4. These are in good agreement with crystal structures of AAF (Van Meerssehe et al., 1980) and some of its hydroxylated derivatives (Neidle et al., 1981) that have been solved since this work was initiated.

Table II: Fluorene–Cytidine Stacked Minimum Energy Conformations of dCpdG-C8(G)-N2(AAF)[a]

conformer	ΔE	χ'	ψ_1	ϕ'	ω'	ω	ϕ	ψ	χ	P_1	P_2	α	β	γ	δ	ω',ω,ψ
1	0	48	56	267	85	87	238	190	240	162	160	97	−77	−3	66	g^+g^+t
2	0.5	36	178	196	170	319	107	69	235	39	180	107	270	−8	85	tg^-g^+
3	1.9	60	179	207	330	106	197	163	248	50	176	93	300	−2	63	g^-g^+t
4	2.2	47	178	195	49	259	156	59	237	39	18	69	48	13	42	$g^+g^-g^+$
5	3.7	48	177	182	34	95	217	193	241	166	22	73	48	13	43	g^+g^+t
6	4.2	34	183	182	55	61	191	171	254	48	35	101	308	−7	−49	g^+g^-t
7	5.2	139	57	280	177	76	250	188	241	162	144	97	295	−4	67	tg^+t

[a] Torsion angles given in deg and energies, ΔE, in kcal/mol. The domains g^+, t, and g^- are centered at 60°, 180°, and 300°, respectively. Minima with energies to about 5 kcal/mol are listed. Only the lowest energy α, β, and γ combinations are given.

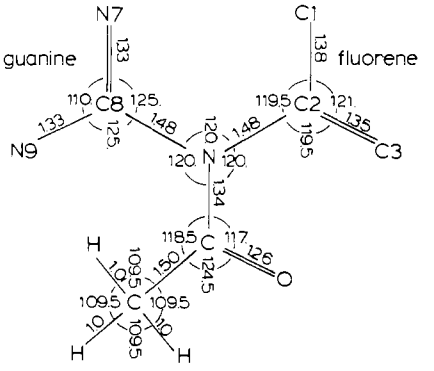

FIGURE 4: Bond lengths and angles assigned to C8(G)-N2(AAF) linkage site.

The energy was calculated for the interaction of each atom with every other atom, excluding those interactions where the interatomic distance is invariant with conformation. All eight DNA backbone torsion angles plus the two pseudorotation parameters, and all torsions at the carcinogen–DNA linkage site (α, β, γ, δ), were flexible parameters. The energy was minimized by a modified version of the Powell algorithm (Powell, 1964). Minimizations were carried to an accuracy of 1° in each parameter at the minimum, with no angle permitted to vary by more than 100° at any step.

Starting conformations were the following combinations: for χ', anti 15° (C-3′ endo), 55° (C-2′ endo); for χ, syn 240°; for P_1, P_2, 18° (C-3′ endo), 162° (C-2′ endo). For the ω',ω,ψ combination, all the minimum energy regions of dCpdG (B. Hingerty and S. Broyde, unpublished results) and other deoxydinucleoside monophosphates (Broyde et al., 1978) below 5 kcal/mol were investigated. These are the following: ψ = 60°, ω',ω = 60°, 180°; 60°, 290°; 180°, 290°; 290°, 180°; 290°, 290°; ψ = 180°, ω',ω = 60°, 60°; 180°, 60°; 290°, 60°; 290°, 180°; ψ = 300°, ω',ω = 60°, 290°; 290°, 60°; 290°, 290°. ψ_1 was flexible but equal to ψ in the initial trials. Its optimum staggered conformation was subsequently computed for minimum energy conformers below ΔE = 5 kcal/mol. Starting conformations for α and β were ±45°, γ was started at 180°, by analogy with the planar peptide linkage, and δ was started at 60°. The minimum energy conformers below 5 kcal/mol obtained from this search were then used in a second series of trials with γ = 0°, and a third series of trials was subsequently made to optimize ψ_1. Although model building (Grunberger & Weinstein, 1979) and NMR studies (Evans et al., 1980; Leng et al., 1980; Santella et al., 1980) have strongly suggested that the guanine is syn in the C8(G)-N2-(AAF) adduct with DNA, we decided to make a restricted search of the anti domain after experiments (Evans et al., 1980; Leng et al., 1980) and computations for the deacetylated C8(G)-N2(AF) adduct (B. Hingerty and S. Broyde, 1982 and unpublished results) had shown plausible anti conformers, despite the fact that linkage was at guanine C-8, which predisposes guanines to be syn for steric reasons. The 21 anti conformations below 3 kcal/mol computed for the deacetylated dCpdG-C8(G)-N2(AF) were used as starting conformers in a search for dCpdG-C8(G)-N2(AAF) anti minima. In these trials α and β were started at ±90°, since experience had shown these values were better than ±45°, used previously.

Molecular models were constructed from MDI/Academic Press Components.

Results and Discussion

Conformations with Fluorene–Cytidine Stacking: A Fluorene Intrastrand Stack Model. Because of the large number of variables, more than 50 minimum energy conformations were computed below 5 kcal/mol. In order to present a meaningful selection, we are showing only the lowest energy conformation of γ. However, it should be borne in mind that each local minimum has an analogue with γ near 180° (and, hence, the acetyl reversed) which is close in energy. Similarly, where conformers were computed that differed only in α and β such that the fluorene is rotated 180° about its long axis, only the lowest energy form is presented, unless the difference appears significant.

Three types of conformers differing in overall aspect were computed with energies less than 5 kcal/mol. Most important are forms in which the fluorene is stacked approximately coplanar with cytidine, the guanine is syn, and the plane of the guanine is twisted nearly perpendicular to the plane of the fluorene (Figure 5 and Table II). Five totally different ω',ω,ψ combinations produced such base displaced forms, including the global minimum and the second lowest energy conformation with ΔE = 0.5 kcal/mol. In relation to these results, it is interesting that a polycyclic aromatic carcinogen–nucleoside adduct whose crystal structure has been solved has the base (adenine) syn and nearly perpendicular to the polycyclic aromatic moiety (Carrell et al., 1981). A recent force field conformational analysis of deoxyguanosine C-8 substituted AAF shows the guanine to be syn and twisted as well (Lipkowitz et al., 1982). The global minimum occupies conformational regions similar to the dCpdG segment of Z-DNA (ω',ω,ψ = g^+,g^+,t) except that the pucker of the guanine-linked deoxyribose, P_1, is in the C-2′-endo domain, while the Z form has P_1 in the C-3′-endo region. Higher energy variants of this conformation with both deoxyribose puckers C-3′ endo or with P_1 C-2′ endo and P_2 C-3′ endo are of similar appearance. (The terms C-3′-endo and C-2′-endo domain designate a range of conformers with P in the 0°–60° and 140°–200° sections of the pseudorotation circle, respectively.) The Z-like global minimum is plausible for random sequence DNA modified at a dCpdG subunit.

The second lowest energy conformation also has fluorene–cytidine stacking. Its backbone conformation resembles a fiber diffraction model (Arnott et al., 1980) and segments of crystalline (Drew et al., 1981) B-DNA with ω',ω,ψ = t,g^-,g^+.

Table III: Fluorene Intrastrand Stacked Conformation of $d(G_1pC_2pG_2pC_3)$ Modified with AAF at G_2[a]

	χ'	ϕ'	ω'	ω	ϕ	ψ	χ	P_1	P_2	α	β	γ	δ
$d(G_1pC_2)$	57	279	145	278	165	38	48	160	162				
$d(C_2pG_2)$	48	267	85	87	238	190	240	162	160	97	77	−3	66
$d(G_2pC_3)$	240	273	287	280	182	48	37	165	162				

[a] Torsion angles are given in deg.

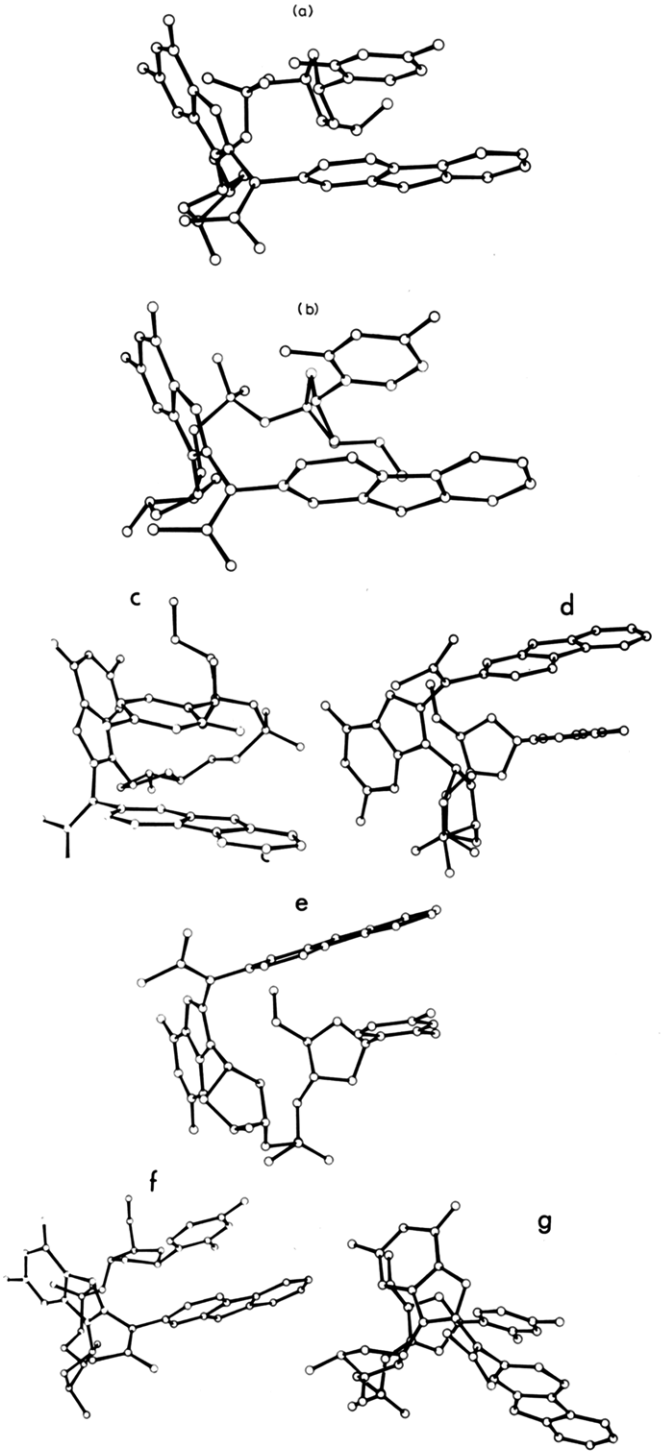

FIGURE 5: Fluorene–cytidine stacked minimum energy conformations of dCpdG-C8(G)-N2(AAF). (a) and (b) are conformers 1 and 2 of Table II. (c)–(g) are conformers 3–7.

However, it differs in the guanine glycosidic torsion which is anti in the B form and in the guanine-linked deoxyribose which is C-2′-endo domain in the B form and C-3′-endo domain in the fluorene–cytidine stacked conformation. This B-like fluorene base stacked conformation may occur in random sequence DNA modified at a site other than a dCpdG subunit.

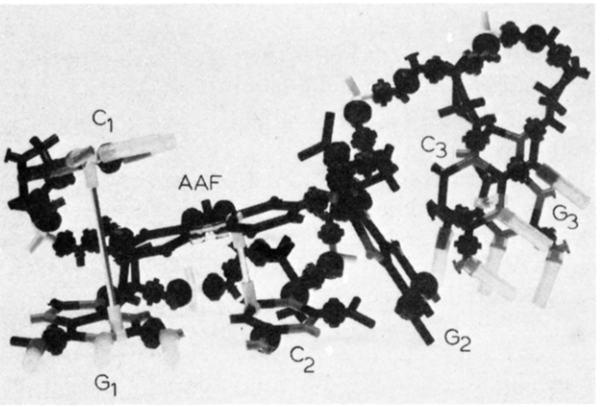

FIGURE 6: Fluorene intrastrand stack model for AAF modification of DNA incorporating the global minimum: conformer 1 of Table II. See text.

Model building indicates that these computed conformations are sufficiently different from the B form that they cannot be fitted directly into it without conformational distortion to the adjacent sites on the same strand. The effect on the two immediately neighboring sites, whose sequence is dGpdC, was investigated for the global minimum. Two energy minimizations were made for dGpdC. In these trials, the guanine- or cytidine-linked glycosidic torsions and deoxyribose puckers were fixed to their values at the dCpdG adduct site, while the other variables were started in the B form (Arnott et al., 1980). In this way the flexible parameters at the dGpdC adjacent sites could take up any strain engendered by the conformational requirements of the adduct site. Conformational angles for this energy-minimized single-stranded tetramer, $d(G_1pC_2pG_2pC_3)$, are given in Table III. A hexameric $(dCpdG)_3$ model incorporating this tetramer is shown in Figure 6. It has a B form subunit $d(C_3pG_3)$, added in the 3′-linked direction, where no interference from AAF occurs. In the 5′-linked direction the wide AAF is also stacked with the guanine G_1 of the $d(G_1pC_2)$ adjacent site. In this direction, B form cannot be added to the next neighboring site without some modification. An intriguing possibility, suggested by the model, is that AAF may intercalate between the bases of a slightly modified B form at this next neighbor $d(C_1pG_1)$ position. A final modified B form $d(C_1pG_1)$ residue has been added to the model, in which the bases have been expanded to 6.8 Å, to accommodate the intercalating AAF. One six-membered ring of the AAF is now stacked between cytidine and guanine of this terminal $d(C_1pG_1)$ residue, while the other six-membered ring, at the linkage site, is stacked with cytidine of the $d(C_2pG_2)$ modified residue on the same strand. The model shows a severe bend or kink in the B-type helix induced by the AAF, whose plane is perpendicular to the helix axis of one arm. This model may reconcile the experimental findings that AAF induces "hinge points" in DNA, as evidenced by reduced viscosity and radius of gyration (Fuchs & Daune, 1972), while an electric dichroism measurement (Fuchs et al., 1976) indicated that the fluorene ring in AAF-modified DNA is nearly perpendicular to the helix axis. Stacking between the wide AAF with three bases on the same strand

is consistent with CD data (Fuchs & Daune, 1972), suggesting base–fluorene interaction. Experimental findings on the number of base pairs ruptured per modified site vary widely depending on conditions, with reports ranging from 1 to 50 (Fuchs & Daune, 1972, 1974; Yamasaki et al., 1977). In our model the complementary strand must undergo a severe distortion of unknown conformation. Consequently, it is difficult to assess the number of ruptured base pairs. However, only the two bases at the modified dCpdG unit are clearly excluded from base pairing, although further disruption especially in the 5′-linked direction would not be at all surprising.

The concept of covalent intercalation was first introduced by Shapiro and Klein in 1967. Models for covalent intercalation of AAF (Drinkwater et al., 1978) and benzo[*a*]pyrene diol epoxide (Drinkwater et al., 1978; Frenkel et al., 1978; Hogan et al., 1981) modified DNA subunits have recently been presented. The model of Hogan et al. (1981) specifically suggests a bend in the helix axis. The Drinkwater model differs from ours in overall aspect in that intercalation of the AAF occurs at the modification site rather than beyond it. Intercalation of a base between distant residues is found in yeast phenylalanine tRNA where G18 intercalates between G57 and m^1A58 (Jack et al., 1976).

The other computed fluorene–cytidine stacked conformations have backbone torsion angles that have not been observed for DNA helices. [The ω',ω,ψ combination t,g^+,t of conformer 7, Table II, is found as a nonintertwining base-paired duplex in DNA fibers saturated with an intercalating molecule, but this duplex has alternating sugar pucker (Arnott & Chandrasekaran, 1981).] These combinations are even higher in energy when 3′- and 5′-terminal phosphates are added to dinucleoside monophosphates (Broyde & Hingerty, 1979; Olson, 1981). However, similar ω',ω,ψ combinations exist in the loop regions of yeast phenylalanine tRNA (Hingerty et al., 1978; Holbrook et al., 1978), where compensating tertiary interactions are present. Their presence in the loops reinforces the conclusion that fluorene intrastrand stacking induces a bend or kink.

The large number of fluorene–cytidine stacked low-energy conformers computed for dCpdG-C8(G)-N2(AAF), including the global minimum and the second lowest energy conformation, indicates that this is a highly probable mode of interaction of AAF with polynucleotides, as inferred from model building and experiment (Grunberger & Weinstein, 1979). These conformers are sufficiently near one another in energy that any, or even all of them, might occur under different conditions, such as a change in the nature of the adjacent base, the level of modification, or the salt concentration. Thus, base displacement is likely to represent a variety of conformations, just as is the case for base stacking (Broyde et al., 1978). The different fluorene intrastrand stacked conformations might have different effects on the adjacent sites on the same strand, and on the opposite strand. This may explain, in part, why such a large range of base pairs can be destabilized by a single AAF modification.

Forms with Guanine–Cytidine Stacking and AAF at the Helix Interior: An Internal Fluorene Model. A second group of low-energy conformers has the guanine syn and the fluorene plane nearly perpendicular to the plane of guanine. However, approximate stacking or coplanarity exists between guanine and cytidine, rather than between fluorene and cytidine. The fluorene is situated so that it obstructs the cytidine base-pairing sites. The lowest energy conformer of this group with ΔE = 0.7 kcal/mol has $\omega',\omega,\psi = g^-,g^-,g^+$, as in the A and B forms. The deoxyribose pucker in this conformer is mixed C-2′ endo(C)–C-3′ endo(G), but higher energy analogues of similar appearance do not have mixed pucker. Again, a number of different ω',ω,ψ combinations, listed in Table IV and shown in Figure 7, have similar features.

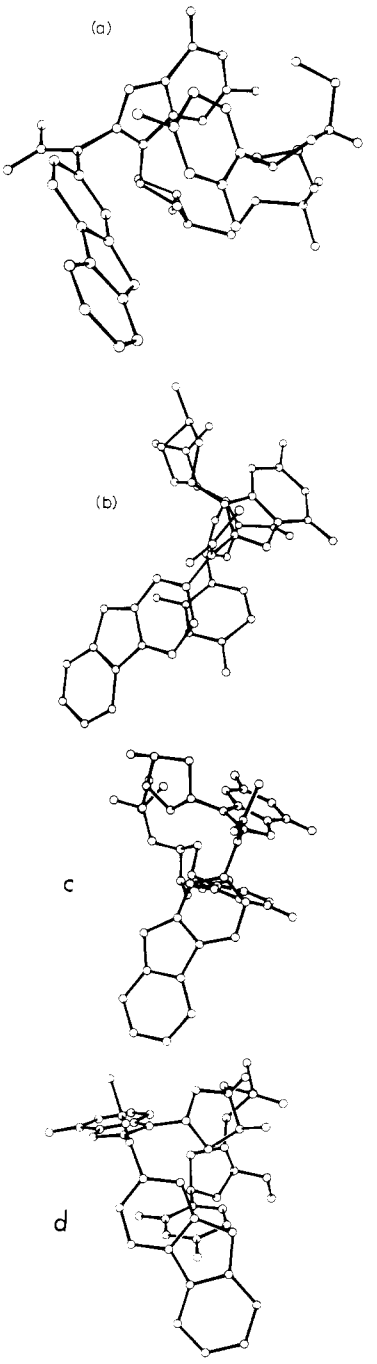

FIGURE 7: Guanine–cytidine stacked minimum energy conformations of dCpdG-C8(G)-N2(AAF). (a) and (b) are two views of conformer 1 (Table IV). (c) and (d) are conformers 2 and 6, respectively.

The lowest energy form of this type was incorporated into a model of duplex $(dCpdG)_3$ in which all the other residues were B form (Figure 8). This was possible without damage to adjacent sites on the same strand. The modified guanine is rotated to the helix exterior. The AAF is inside the helix, directly between the base pair that would otherwise be formed between cytidine of the substituted dCpdG unit and the guanine of the opposite strand. The long axis of the fluorene makes an angle of about 50° with the average position of the helix axis. The two base pairs of the altered dCpdG segment and probably the base pair above are ruptured. This con-

Table IV: Guanine–Cytidine Stacked Minimum Energy Conformations of dCpdG-C8(G)-N2(AAF) with Internal Fluorene[a]

conformer	ΔE	χ'	ψ_1	ϕ'	ω'	ω	ϕ	ψ	χ	P_1	P_2	α	β	γ	δ	ω',ω,ψ
1	0.7	57	56	208	308	240	177	61	243	44	159	97	290	−1	−55	g^-,g^-,g^+
2	1.5	52	53	180	268	151	178	179	238	162	161	98	284	−5	68	g^-,t,t
3	1.7	51	59	196	296	282	176	58	239	47	36	106	74	−5	79	g^-,g^-,g^+
4	2.3	58	56	186	268	286	177	54	244	98	154	100	91	−2	68	g^-,g^-,g^+
5	2.3	235	58	202	295	280	175	55	239	49	56	100	112	−3	70	g^-,g^-,g^+
6	3.8	37	180	252	313	304	171	304	230	165	106	278	104	−3	66	g^-,g^-,g^-
7	4.1	52	59	194	305	172	180	171	243	165	34	5	283	−1	−57	g^-,t,t

[a] See footnote to Table II.

Table V: Guanine–Cytidine Stacked Minimum Energy Conformations of dCpdG-C8(G)-N2(AAF) with External Fluorene[a]

conformer	ΔE	χ'	ψ_1	ϕ'	ω'	ω	ϕ	ψ	χ	P_1	P_2	α	β	γ	δ	ω',ω,ψ
1	3.4	40	172	283	90	52	196	174	252	47	180	96	−66	−1	63	g^+,g^+,t
2	4.8	39	174	282	89	53	196	174	250	47	180	98	109	0	65	g^+,g^+,t
3	5.8	41	166	284	92	47	194	169	247	46	181	44	49	16	35	g^+,g^+,t
4	4.4	35	182	193	170	53	252	182	243	43	169	100	288	−2	68	t,g^+,t

[a] See footnote to Table II.

formation does not severely distort the normal helix direction by creating a kink. Rather, a very gentle bend is induced in the helix axis. Since the AAF interacts with the opposite strand in this model, energy calculations considering both strands might lead to some conformational adjustments (possibly fluorene interstrand stacking). However, its overall aspect with an internal fluorene appears to be feasible.

A number of experimental results suggest that the major adduct of AAF with DNA can cause more than one type of conformational distortion, depending on conditions. The internal fluorene model may further explain some of the observed variety in duplex destabilization by AAF. An electric dichroism investigation by Chang and co-workers (1974) revealed an angle of 60° between the plane of the fluorene and the helix axis in AAF-modified DNA. This conflicts with the 80° value of Fuchs et al. (1976), suggesting fluorene base stacking, but agrees better with our internal fluorene model. Since very different conditions were employed in the two studies, it is possible that denaturation without fluorene intrastrand base stacking was observed by Chang et al., while Fuchs and co-workers did observe such stacking. Recent in vivo studies indicate that about 15% of the C8(G)-N2(AAF) adducts are persistent, while the remainder are repaired (Visser & Westra, 1981). This suggests that there may be two types of conformational distortions in mixed sequence DNA, a severe alteration that is repaired, which can be visualized by the fluorene intrastrand stack model (Figure 6), and a more subtle modification, represented by the internal fluorene model shown in Figure 8, which escapes repair. An approximate evaluation of the statistical weights (Olson, 1975) associated with fluorene base-stacked conformers 1 and 2 (Table II) and AAF inserted conformer 1 (Table IV) yields probabilities of 57.7%, 24.7%, and 17.6%, respectively, assuming contributions by only these three conformers, assigning them equal entropies, and using the energies given in the tables. The combined 82.4% contribution by the fluorene base-stacked forms and the 17.6% contribution by the internal fluorene form is suggestive of the experimental finding that 15% of the adducts are persistent while the remainder are repaired. However, the agreement may be coincidental, since repair is a complex process which can vary from one system to another.

Outside Bound Forms with Guanine–Cytidine Stacking: The Z Form. A third group of important low-energy minima maintains guanine–cytidine stacking while placing the fluorene

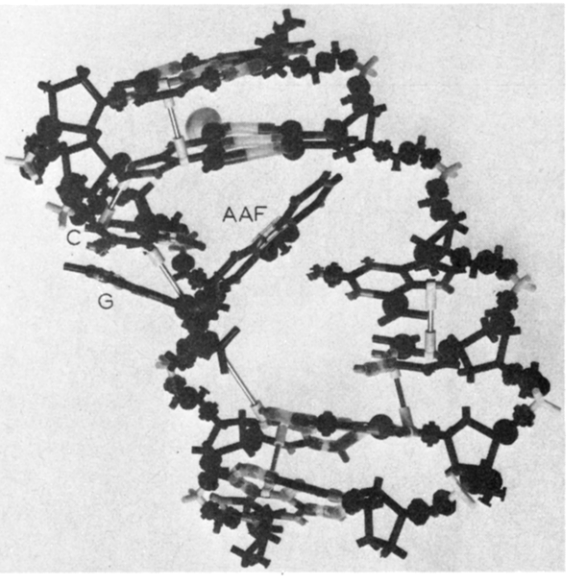

FIGURE 8: Internal fluorene model for AAF modification of DNA. Conformer 1 of Table IV is incorporated in a B-form hexameric duplex $(dCpdG)_3$.

in a location where base pairing is not obstructed. Most important are conformations very similar to the dCpdG segment of Z_I-DNA (Wang et al., 1981) with $\omega',\omega,\psi = g^+,g^+,t$ and deoxyriboses alternately C-3′ endo(G)–C-2′ endo(C). They are listed in Table V (conformers 1, 2, and 3) and shown in Figure 9. These conformers differ from each other in α and β, which determine the orientation of the fluorene. Conformer 2 differs from conformer 1 in that the fluorene is rotated 180° about its long axis and is not shown in the figure. The calculated structures fit readily into the Z_I-DNA double helix. Figure 10 shows the computed adduct of Figure 9a inserted into a model of the Z_I-DNA tetrameric duplex dGpdCpdGpdC, in the place of a dCpdG segment. The AAF is located on the outside of this double helix and induces little strain or distortion. Because of its position at the helix exterior, the AAF has the possibility of being flexible, its orientation able to vary in α and β as shown in Figure 9. Considerable experimental evidence is at hand indicating that AAF-modified duplex poly(dC-dG) can adopt the Z-DNA conformation exemplified by this structure (Sage & Leng, 1980; Santella et al., 1981a,b).

Table VI: Guanine Anti Minimum Energy Conformation of dCpdG-C8(G)-N2(AAF)[a]

conformer	ΔE	χ'	ψ_1	ϕ'	ω'	ω	ϕ	ψ	χ	P_1	P_2	α	β	γ	δ	ω',ω,ψ
1	1.9	76	59	206	294	205	187	63	−20	144	33	93	−138	10	−64	g^-,t,g^+

[a] See footnote to Table II.

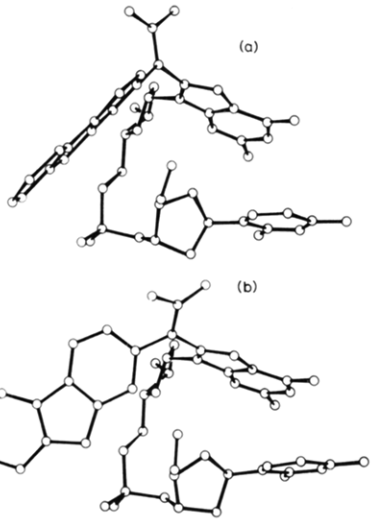

FIGURE 9: Z-form minimum energy conformations of dCpdG-C8-(G)-N2(AAF). (a) and (b) are conformers 1 and 3 of Table V.

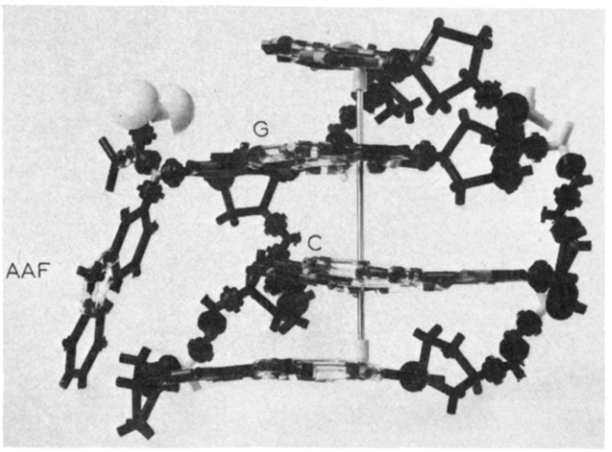

FIGURE 10: Z-form model for AAF modification of DNA. Conformer 1 of Table V is incorporated into Z-form duplex d(CpGpCpG).

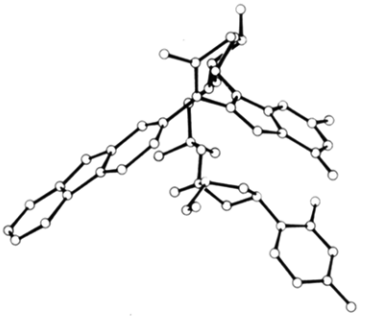

FIGURE 11: Outside bound minimum energy conformer 4 of Table V of dCpdG-C8(G)-N2(AAF).

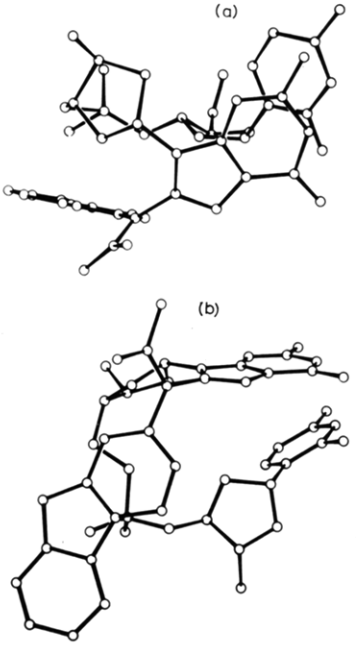

FIGURE 12: Two views of guanine anti minimum energy conformation of dCpdG-C8(G)-N2(AAF) listed in Table VI.

A second type of conformer with similar appearance (Table V, conformer 4, and Figure 11) has the ω',ω,ψ combination t,g^+,t with alternating pucker C-3′ endo(G)–C-2′ endo(C). Interestingly, this conformational combination is observed in DNA fibers saturated with an intercalating molecule (Arnott & Chandrasekaran, 1981).

Anti Guanine Conformation. While 81 trials were made with guanine anti, only one anti conformation with energy below 5 kcal/mol was found. This, in itself, indicates that the syn domain is preferred. However, the fact that a low-energy anti conformation was computed calls attention to its possibility, and there may be others. A full theoretical survey of the anti domain has been made; no additional conformers below 5 kcal/mol were found. The anti conformation is at an energy of only 1.9 kcal/mol and has the ω',ω,ψ combination g^-,t,g^+ (Table VI), with the guanine glycosidic torsion at the abnormally low value of −20°. Glycosidic torsions associated with C-2′-endo puckering (P_1) are usually about 60°–100° higher (Sundaralingam, 1975). In other respects, however, this anti conformer is quite normal. As shown in Figure 12, guanine–cytidine stacking is preserved, and the AAF is again nearly perpendicular to guanine. However, the base-pairing sites are not obstructed by the AAF in this dCpdG residue, although the AAF may interfere with base pairing at adjacent sites. The g^-,t,g^+ combination is found at the turn of the anticodon and the TψC loop of yeast phenylalanine tRNA (Kim & Sussman, 1976; Sundaralingam et al., 1976). Consequently, this modified conformer would likely bend a normal A or B helix.

Sugar Pucker. An interesting observation is the importance of the deoxyribose pucker in determining the overall appearance of AAF-modified dCpdG. The greatest difference between the global minimum fluorene base-stacked conformation and the Z_I-DNA outside bound form is in the pucker of the guanine-linked deoxyribose, which is C-3′ endo in the Z form and C-2′ endo in the fluorene base-stacked form. The global minimum, with AAF stacked on cytidine, can be converted primarily by an alteration in sugar pucker, together with some adjustments within each torsional domain (compare conformer 1 in Tables II and V) to the Z form with its G–C stack and

AAF at the helix exterior. Similarly the fluorene base-stacked t,g^+,t conformer 7 of Table II, with P_1 and P_2 C-2′ endo, is converted to the outside bound form, conformer 4 of Table V, by conversion of P_1 to C-3′ endo, together with large adjustments in χ' and ϕ'. Another interesting point about the sugar pucker adjacent to the modified guanine is its tendency to verge from the classical C-3′-endo region centered at P = 0° toward the "eastern" region of the pseudorotation circle. The tendency for unusual nucleosides to occupy the "e" domain near P = 90°, between C-3′ endo and C-2′ endo, has been noted by Olson (1982).

Correlated Motions. A repeated theme in the computed conformations is their grouping into types with similar overall appearances, either G–C stack or fluorene–cytidine stack, with totally different DNA backbone conformations, even within each group. This similar aspect with different conformations is due to the crankshaft-like motions of non-nearest-neighbor torsions (Olson, 1981). These motions permit stacking, the energetic driving force, in a large variety of conformational combinations, by compensatory rotations in opposite directions of one or more pairs of nonadjacent bonds. A study of these motions is in progress.

Conclusion

Three types of low-energy syn guanine conformers have been computed for the C8(G)-N2(AAF) adduct of dCpdG with AAF. All three types of conformations have the guanine nearly perpendicular to AAF. (1) One type has the fluorene–cytidine base-stacked forms which cause a severe distortion at the site of the lesion and adjacent to it when incorporated into a normal B-type helix, akin to the single-stranded bend regions observed in tRNA. This is the most favored conformation. (2) Another type has conformations in which guanine–cytidine stacking is maintained and AAF is in a base-pair obstructing position. When incorporated into a B-form duplex, base pairing at and near the modification site is disrupted by the AAF moiety, which is located inside the helix between the base pairs, while the guanine is at the helix periphery. However, major distortion in helix direction, such as a kink, is not engendered. The two models of larger polymers assume that the sites adjacent to the modification are similar to the B form. This seems reasonable for random sequence DNA at the low levels of modification which are biologically relevant. (3) The third type has outside bound conformations in which the AAF is external to left-handed Z-DNA, or to an alternate helix, in a somewhat flexible situation. In addition, a low-energy anti conformation was computed which would bend the normal A or B helix.

Experimental results indicate that AAF can induce a base-paired left-handed conformation when linked to duplex poly(dC-dG). This may well be the Z form. In studies with certain dinucleoside monophosphates, CD and NMR results have suggested overlap between fluorene and the adjacent base, which led to the base displacement model. Other work with mixed sequence DNA has revealed denaturation caused by AAF, which led to the insertion–denaturation concept. Base displacement and insertion–denaturation have been understood to refer to the same conformational distortion, whose details, other than that the guanine is syn, are unknown. Our results suggest a preferred fluorene intrastrand base-stack model which causes a severe change in helix shape (Figure 6), while an internal fluorene structure (Figure 8) causes little distortion in helix direction. Ross et al. (1982) have recently shown that AAAF adducts to DNA in chromatin do not cause the major distortion seen in protein free DNA. The recent finding that about 15% of the C8(G)-N2(AAF) adducts occurring in vivo remain persistently bound also supports the view that this adduct may induce more than one type of conformational distortion in mixed sequence DNA. The severe distortion produced by fluorene intrastrand stacking may be repaired, while the smaller change induced by an internal fluorene model could escape the repair mechanism.

Acknowledgments

We thank Professor Robert Shapiro, Chemistry Department, New York University, for suggesting this problem and for many helpful discussions.

References

Altona, C., & Sundaralingam, M. (1972) *J. Am. Chem. Soc. 94*, 8205–8212.

Arnott, S., & Chandrasekaran, R. (1981) *Biomolecular Stereodynamics, I* (Sarma, R., Ed.) pp 99–122, Adenine Press, New York.

Arnott, S., Dover, S., & Wonacott, A. (1969) *Acta Crystallogr., Sect. B 25B*, 2192–2206.

Arnott, S., Chandrasekaran, R., Birdsall, D., Leslie, A., & Ratliff, R. (1980) *Nature (London) 283*, 743–745.

Broyde, S., & Hingerty, B. (1979) *Nucleic Acids Res. 6*, 2165–2178.

Broyde, S., & Hingerty, B. (1981) *Biomolecular Stereodynamics, II* (Sarma, R., Ed.) pp 455–467, Adenine Press, New York.

Broyde, S., & Hingerty, B. (1982) *Chem.-Biol. Interact.* (in press).

Broyde, S., Wartell, R., Stellman, S., & Hingerty, B. (1978) *Biopolymers 17*, 1485–1506.

Burns, D., & Iball, J. (1955) *Proc. R. Soc. London, Ser. A A227*, 200–215.

Carrell, H., Glusker, J., Moschel, R., Hudgins, W., & Dipple, A. (1981) *Cancer Res. 41*, 2230–2234.

Chang, C., Miller, S., & Wetmur, S. (1974) *Biochemistry 13*, 2142–2148.

Drew, H., Wing, R., Takano, T., Broka, C., Tanako, T., Itakura, K., & Dickerson, R. (1981) *Proc. Natl. Acad. Sci. U.S.A. 78*, 2179–2183.

Drinkwater, N., Miller, J., Miller, E., & Yang, N. (1978) *Cancer Res. 38*, 3247–3255.

Evans, F., Miller, D., & Beland, F. (1980) *Carcinogenesis (N.Y.) 1*, 955–959.

Evans, J. (1960) *Spectrochim. Acta 16*, 428–442.

Frenkel, K., Grunberger, D., Boublik, M., & Weinstein, I. (1978) *Biochemistry 17*, 1278–1282.

Fuchs, R. P. P. (1975) *Nature (London) 257*, 151–152.

Fuchs, R. P. P., & Daune, M. (1972) *Biochemistry 11*, 2659–2666.

Fuchs, R. P. P., & Daune, M. (1974) *Biochemistry 13*, 4435–4440.

Fuchs, R. P. P., Lefevre, J., Pouyet, J., & Daune, M. (1976) *Biochemistry 15*, 3347–3351.

Grunberger, D., & Weinstein, I. (1979) *Chemical Carcinogens and DNA* (Grover, P. L., Ed.) pp 59–93, CRC Press, Boca Raton, FL.

Grunberger, D., & Santella, R. (1981) *ICN-UCLA Symposium on Mechanisms of Chemical Carcinogenesis*, Alan R. Liss, Inc., New York.

Grunberger, D., Nelson, J., Cantor, C., & Weinstein, I. (1970) *Proc. Natl. Acad. Sci. U.S.A. 66*, 488–494.

Hingerty, B., & Broyde, S. (1982) *Int. J. Quantum Chem.* (in press).

Hingerty, B., Brown, R., & Jack, A. (1978) *J. Mol. Biol. 124*, 523–534.

Hogan, M., Dattagupta, N., & Whitlock, J. (1981) *J. Biol. Chem. 256*, 4504–4513.
Holbrook, S., Sussman, J., Warrant, R., & Kim, S.-H. (1978) *J. Mol. Biol. 123*, 631–660.
Howard, P., Casciano, D., Beland, F., & Shaddock, J. (1981) *Carcinogenesis (N.Y.) 2*, 97–102.
Irving, C., & Veazey, R. (1969) *Cancer Res. 29*, 1799–1804.
Jack, A., Ladner, J., & Klug, A. (1976) *J. Mol. Biol. 108*, 619–649.
Kao, J., & Allinger, N. (1977) *J. Am. Chem. Soc. 99*, 975–986.
Kapuler, A., & Michelson, A. (1971) *Biochim. Biophys. Acta 232*, 436–450.
Kim, S.-H., & Sussman, J. (1976) *Nature (London) 260*, 645–646.
Kriek, E. (1972) *Cancer Res. 32*, 2042–2048.
Kriek, E. (1974) *Biochim. Biophys. Acta 355*, 177–203.
Kriek, E., & Reitsema, J. (1971) *Chem.-Biol. Interact. 3*, 397–400.
Kriek, E., & Westra, J. (1980) *Carcinogenesis (N.Y.) 1*, 459–468.
Kriek, E., Miller, J., Juhl, U., & Miller, E. (1967) *Biochemistry 6*, 177–182.
Lakshminarayanan, A., & Sasisekharan, V. (1969a) *Biopolymers 8*, 475–488.
Lakshminarayanan, A., & Sasisekharan, V. (1969b) *Biopolymers 8*, 489–503.
Leng, M., Ptak, M., & Rio, P. (1980) *Biochem. Biophys. Res. Commun. 96*, 1095–1102.
Levine, A., Fink, L., Weinstein, I., & Grunberger, D. (1974) *Cancer Res. 34*, 319–327.
Lipkowitz, K., Chevalier, T., Widdifield, M., & Beland, F. (1982) *Chem.-Biol. Interact.* (in press).
Momany, F., McGuire, R., Burgess, A., & Scheraga, H. (1975) *J. Phys. Chem. 79*, 2361–2381.
Neidle, S., Subbiah, A., Mason, A., & Islam, S. (1981) *Carcinogenesis (N.Y.) 2*, 901–907.
Olson, W. (1975) *Biopolymers 14*, 1775–1795.
Olson, W. (1981) *Biomolecular Stereodynamics, I* (Sarma, R., Ed.) pp 327–344, Adenine Press, New York.
Olson, W. (1982) *J. Am. Chem. Soc. 104*, 270–286.
Ornstein, R., & Rein, R. (1979) *Biopolymers 18*, 1277–1291.
Powell, M. (1964) *Comput. J. 7*, 155–159.
Renugopalakrishnan, V., Lakshminarayanan, A., & Sasisekharan, V. (1971) *Biopolymers 10*, 1159–1167.
Ross, J., Metzger, G., & Werbin, H. (1982) *Biochemistry 21*, 1369–1374.
Sage, E., & Leng, M. (1980) *Proc. Natl. Acad. Sci. U.S.A. 77*, 4597–4601.
Santella, R., Kriek, E., & Grunberger, D. (1980) *Carcinogenesis (N.Y.) 1*, 897–902.
Santella, R., Grunberger, D., Weinstein, I. B., & Rich, A. (1981a) *Proc. Natl. Acad. Sci. U.S.A. 78*, 1451–1455.
Santella, R., Grunberger, D., Broyde, S., & Hingerty, B. (1981b) *Nucleic Acids Res. 9*, 5459–5467.
Sasisekharan, V. (1973) *Jerusalem Symp. Quantum Chem. Biochem. 5*, 247–260.
Scott, R., & Scheraga, H. (1966) *J. Chem. Phys. 44*, 3054–3069.
Shapiro, R., & Klein, R. (1967) *Biochemistry 6*, 3576–3582.
Srinivasan, A., & Olson, W. (1980) *Fed. Proc., Fed. Am. Soc. Exp. Biol. 39*, 2199.
Srinivasan, A., Yathindra, N., Rao, V., & Prakash, S. (1980) *Biopolymers 19*, 165–171.
Sundaralingam, M. (1975) *Structure and Conformation of Nucleic Acids and Protein-Nucleic Acid Interactions* (Sundaralingam, M., & Rao, S., Eds.) University Park Press, Baltimore, MD.
Sundaralingam, M., Mizuno, H., Stout, D., Rao, S., Liebman, M., & Yathindra, N. (1976) *Nucleic Acids Res. 3*, 2471–2484.
Van Meerssehe, M., Germaine, G., Declercq, J., Touillaux, R., Roberfroid, M., & Razzouk, C. (1980) *Cryst. Struct. Commun. 9*, 515–518.
Visser, A., & Westra, J. (1981) *Carcinogenesis (N.Y.) 2*, 737–740.
Wang, A., Quigley, G., Kolpak, F., Van der Marel, G., van Boom, J., & Rich, A. (1981) *Science (Washington, D.C.) 211*, 171–176.
Westra, J., Kriek, E., & Hittenhausen, H. (1976) *Chem.-Biol. Interact. 15*, 149–164.
Yamasaki, H., Leffler, S., & Weinstein, I. B. (1977) *Cancer Res. 37*, 684–691.
Yamasaki, H., Pulkrabek, P., Grunberger, D., & Weinstein, I. B. (1977) *Cancer Res. 37*, 3756–3760.